Thick, Two-Dimensional, Turbulent Boundary Layers Separated by Steps and Slot Jets

RICHARD T. DRIFTMYER*
Naval Ordnance Laboratory, Silver Spring, Md.

The objective of this viscous interaction study was to investigate the separation phenomena which occur ahead of two-dimensional steps and slot jets. This investigation was restricted to the case where the height, h, of the step or jet was less than the boundary-layer thickness, δ. The boundary layer, itself, was turbulent and adiabatic. The independent test variables selected were Re_δ and h/δ. The tests were performed in a two-dimensional, Mach 4.9 half-nozzle boundary-layer channel. Two glass-ported side plates were used to split off the thick sidewall boundary layers. The significance of two parameters, i.e., the Reynolds number and h/δ, was revealed in the study; the degree of influence of either parameter decreased as its value increased. Three useful geometric scaling parameters were defined with the first scaling the initial steep pressure rise region and the second scaling the separation region of the total pressure profile. Use of these two distances permitted the development of a universal pressure profile. The third distance scaled the physical system by defining the standoff position of the separation shock in the freestream.

Nomenclature

b = jet nozzle slot width, in.
D = see Eqs. (5) and (6), in.
F_i = induced force, lbf/unit width
F_j = jet reaction force, lbf/unit width
h = obstruction height, in.
L = length, ft
M = Mach number
P = pressure, psia
Pl = plateau pressure, psia
Re = Reynolds number
T = temperature, °R
XP = separation shock standoff distance, in.
XS = scale change point, in.
ΔXS = initial steep pressure rise distance, in.
$\left(\frac{\Delta XS}{XP}\alpha + \frac{XS}{XP}\beta\right)$ = pressure profile coefficient
$\alpha = \int_{1.0} (P-P_\infty)/(Pl-P_\infty)d(X/\Delta XS)$
$\beta = \int_{1.0} (P-P_\infty)/(Pl-P_\infty)d(X/XS)$
δ = boundary-layer thickness, in.

Subscripts and Superscripts
$*$ = sonic reference
e = exit
j = jet
o = stagnation
s = step
∞ = freestream

Introduction

SUPERSONIC viscous interactions became an important area for study as the need for controlled supersonic flight developed. The simplest control device was the deflected flap which was modeled experimentally as a ramp of various angles. Later on, a more sophisticated control system was developed which used surface jets to deflect the freestream and thereby provide a control force. Fundamental to the general operation of these and other controls, however, is a knowledge of the viscous interactions—the separation and reattachment of the boundary layer—which are complex phenomena usually found to be three-dimensional in nature. Indeed, experimentalists have found the two-dimensional boundary-layer separation extremely difficult—if not impossible—to attain,[1,2] and hence, are forced to accept something less which might better be classified as "pseudo" two dimensional. However, even with this experimental handicap, the knowledge gained in studying such an "almost" two-dimensional separation problem seems to have made the understanding of the more complex three-dimensional separation problems easier, of which there seems to be a multitudinous supply.[3]

Recently Zukoski[4] presented a comprehensive review of turbulent boundary-layer separation ahead of forward-facing steps. He limited his discussion to the two-dimensional problem with turbulent boundary layers where the step height, h_s, exceeded the thickness of the boundary layer, δ. Based upon this review, Zukoski was able to present a very simple force model for step separation where

$$F_{is}/P_\infty h_s = f(M_\infty) \quad (1)$$

Werle[5] also searched the two-dimensional literature where his primary concern was modeling the jet interaction phenomenon. In a subsequent paper,[6,7] Werle et al., compared the step pressure data of Hahn[8] with their jet interaction pressure distributions. Hahn's data covered the Mach number range from 2.5 to 4.0, while the jet interaction data were for Mach 4.0 alone. No significant difference was found to exist between the step-induced or jet-induced separations except locally, in a minor way, near the region of shear layer reattachment. This development of a universal pressure distribution curve resulted by normalizing the pressure rise with the plateau pressure rise, and by normalizing the local distance with the separation distance. Since several step and jet shock heights were involved, as well as a range of Reynolds numbers from 6×10^6/ft to 18×10^6/ft, the independence of the universal pressure distribution with Mach number, Reynolds number, and step or jet height was adequately demonstrated. Indeed, the demonstrated existence of this universal pressure distribution permitted Werle et al., to follow the concept of the step force model developed by Zukoski and obtain similar results for control jets, i.e.,

$$F_{ij}/P_\infty h_j = f(M_\infty) \quad (2)$$

The results expressed by Eqs. (1) and (2) were limited to cases where h exceeded δ. This present paper describes a logical

Received November 30, 1972; revision received August 22, 1973.
Index category: Jets, Wakes, and Viscid-Inviscid Flow Interactions.
* Aerospace Engineer, Applied Aerodynamics Division. Member AIAA.

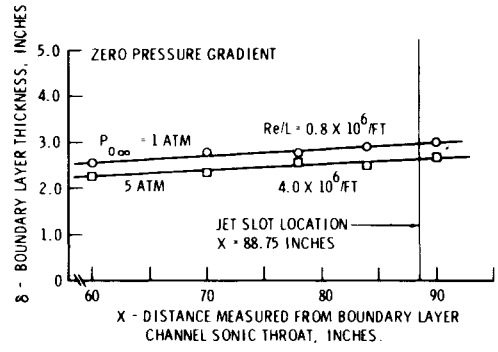

Fig. 1 Boundary-layer thickness distribution along flat test plate.

extension by considering the problem where h is less than δ. The conclusion of this latest study was that Reynolds number effects must be accounted for. That is

$$F_i/P_\infty h = f(M_\infty, h/\delta, Re_\delta) \tag{3}$$

for cases with h less than δ.

Test Equipment and Test Program

The experimental tests were performed in the Naval Ordnance Lab.'s (NOL) Boundary Layer Channel.[9] Figure 1 shows the turbulent boundary-layer thickness distribution, measured along the length of the flat test plate.† The intermediate boundary-layer thicknesses, δ, for $P_{o\infty} = 2$, 3, and 4 atm, were obtained from Fig. 1 by interpolation.

Glass-ported side plates, which were mounted 8 in. apart on the flat side of the two-dimensional wind-tunnel half-nozzle and within the nozzle's exit test rhombus, served to split off the thick sidewall boundary layers. Full-span slot jets and forward-facing steps were positioned between the side plates for testing.

Table 1 presents the step test program and Table 2 presents an outline of the jet interaction test program.

For both the step program and the jet interaction program, adjustments in the test variable, Re_δ (or Re/L in the dimensional form) were easily made by changing the wind-tunnel stagnation pressure. For the step program changes in the dimensionless step height variable, h_s/δ (or simply h_s as presented in Table 1), also proved to be straightforward. The jet shock height, h_j, however, was less amenable to direct control. This problem was handled experimentally during testing by observing the transducer output of a previously selected pressure tap which was located on the flat plate a known distance ahead of the jet slot. It was then a simple matter to increase the jet pressure slowly during the test to locate the start of the separation region's pressure rise at the desired static pressure tap. By selecting different "centerline" pressure taps for different test runs, a reasonable distribution of experimental jet shock heights was thus obtained. The actual jet shock height, h_j, was determined later by direct measurement from photographic data.

Sixty-four static pressure taps were located on the flat test plate ahead of the jet nozzle. The "centerline" pressure distri-

Table 1 Step test program[a]

$Re/L \times 10^{-6}$ (1/ft)	Step height (in.)					
	1.502	1.400	1.205	0.903	0.603	0.247
4.0[b]	x	x	x	x	x	x
3.2	...	x	...	...	...	...
2.4	...	x	...	...	...	...
1.6	...	x	...	...	...	...
0.8	x	x	x	x	x	...

[a] To_j = 590°R.
[b] An oil flow study was conducted for the 4.0 × 10⁶/ft step case only.

† Minor changes in the boundary-layer displacement thickness, due to changes in the wind-tunnel supply pressure, did produce small variations in the test Mach number. These variations in Mach number were accounted for in the data-reduction procedure.

Table 2 Jet interaction test program[a]

$Re/L \times 10^{-6}$ (1/ft)	Jet nozzle configuration sonic nozzles			
	$M_j = 2.89$ $b^* = 0.0335$	$b^* = 0.0157$	$b^* = 0.0299$	$b^* = 0.0599$[b]
4.0	155–78[c]	302–104	157–51	84–28
3.2	157	314	173	...
2.4	157	317–157	173	...
1.6	173	294	186	...
0.8	190–80	364–170	207–110	...

[a] To_∞ = 590°R, To_j = 500°R.
[b] b^*, the sonic reference state (b = throat width in in.).
[c] The range of values of the jet strength, $P_{oj}/P_{o\infty}$.

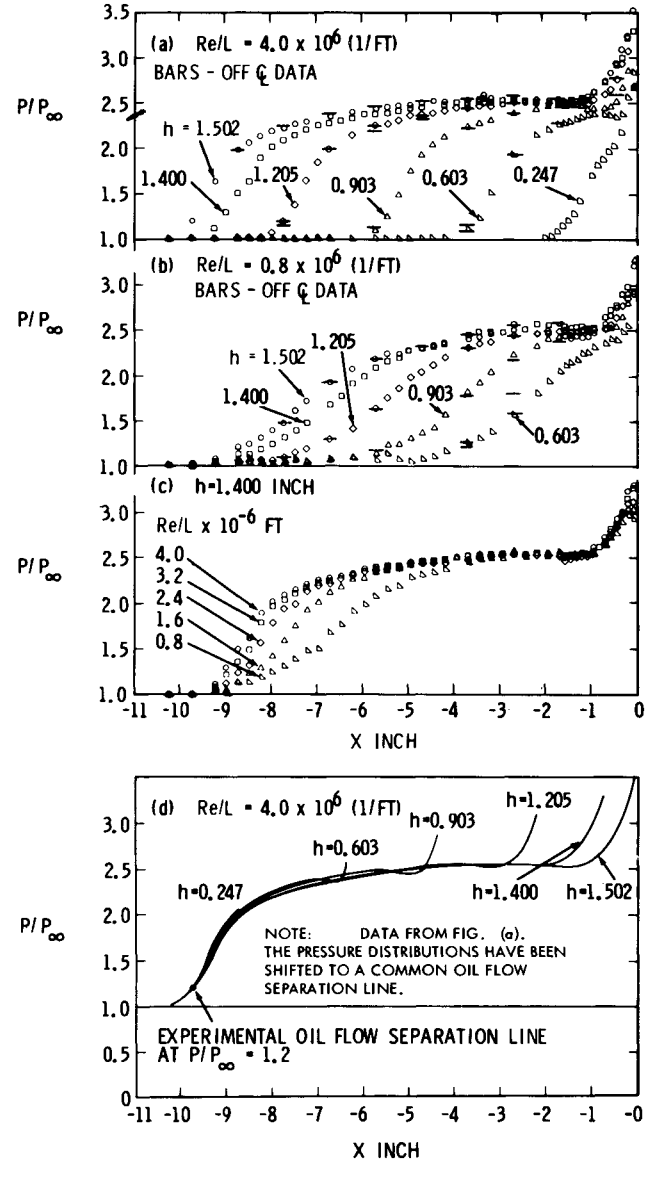

Fig. 2 Step pressure distribution upstream of the step face.

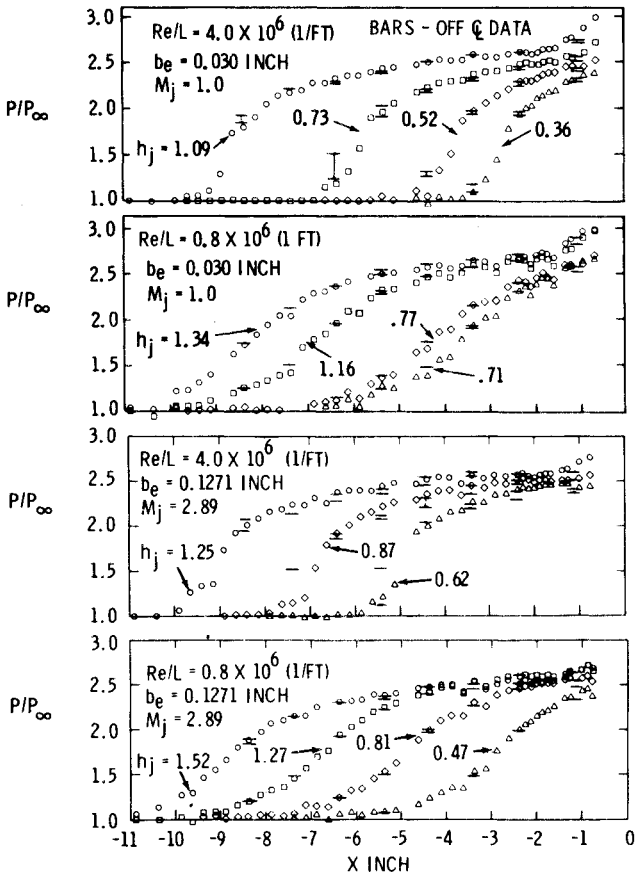

Fig. 3 Jet pressure distributions upstream of the jet nozzle slot.

bution was obtained using 48 pressure taps aligned in a zigzag fashion over the center 2 in. of the 8-in.-wide flow channel as defined by the side plates. The 16 remaining pressure taps, which were located off centerline near the side plates, served to check the two-dimensionality of the flowfield. Some oil flow data, as indicated in Table 1, were also taken as an alternate check on the two dimensionality of the flowfield.[10]

Eight strain-gage pressure transducers, which were directly connected to eight scanner valves, measured the static pressures. Steady-state test conditions were maintained for at least 2 min during which time period the various static pressures were sequentially recorded.

Experimental Results

The primary experimental results were the upstream pressure distributions. These distributions are presented in Fig. 2 for the steps and in Fig. 3 for one sonic and one supersonic interaction jet. Bars shown on these two figures indicate the range of surface pressures measured transverse to the flowfield 2.75 in. on either side of the centerline.

Step Pressure Distributions

Figures 2a, b, and c present three sets of step pressure distributions. Figure 2d shows the data of Fig. 2a, shifted horizontally to a common, experimentally determined oil-flow separation line. Hence, for Fig. 2d only, the step face location, $X = 0$, has meaning for the pressure distribution of the 1.502-in.-high step alone.

The first two pressure distributions shown in Figs. 2a and 2b were obtained at Reynolds numbers per foot of 4.0×10^6 and 0.8×10^6, respectively, for the family of step heights indicated in Table 1. In contrast, Fig. 2c presents data at the constant step height of 1.400 in., taken over the test range of Reynolds number per foot of 4.0×10^6 through 0.8×10^6. As indicated by these data, in Figs. 2a and 2b, the step height influences both the extent of separation and the value of the plateau pressure, Pl, whereas the Reynolds number per foot is observed in Fig. 2c to influence the slope of the pressure profile in the upstream region near the beginning of the pressure rise. The independence of h with the slope of the pressure profile is given in Fig. 2d.

Jet Pressure Distributions

Figure 3 presents four sets of jet interaction pressure distributions. A sonic jet nozzle was used for the first two sets of pressure distributions; a supersonic jet nozzle (Mach = 2.89) was used for the last two sets of pressure distributions. Each set includes data taken at Reynolds numbers per foot of 4.0×10^6 and 0.8×10^6 over a range of jet heights. No significant difference is observed between the sonic and supersonic jet nozzle data. The data in Fig. 3 also appear to be generally consistent with the step data of Fig. 2. Note again that both the extent of separation and the plateau pressure, Pl, vary with the jet height, h_j, and that the influence of Re/L is associated with the initial slope of the pressure profile.

Fluctuations in the Pressure Distributions

It is proper at this time to digress a moment and to comment on the fluctuations observed in the pressure distributions of Figs. 2 and 3. Considerably more pressure fluctuations occurred with the interacting jets than with the steps. The steps, by comparison, provided a fixed corner to which the separated boundary layer could reattach itself. Since the jet is a deformable fluid obstruction, its size is dependent upon both the local, external flowfield properties and the jet supply properties. Of these two influences, maintaining a constant jet supply condition appeared to be the more difficult. Also, within the jet nozzle supply chamber, transverse pressure gradients existed which caused some fluctuations in the jet height along the 8-in. length of the jet nozzle. These fluctuations were observed as double and triple jet shock heights in the high-speed movies taken of the interacting jet.

However, even considering these possibilities for error, the pressure distribution data were found to be quite reasonable and consistent. In the case of steps, repeated runs produced no differences in the pressure distributions.

The Dimensionless Control Force, $F_i/P_\infty h$

The control force results, obtained by integrating the experimental pressure distributions, are presented in Figs. 4 and 5 as a function of h_s/δ and h_j/δ, respectively. The step and jet data exhibit similar trends with Re/L and h/δ, namely, increasing $F_i/P_\infty h$ with increasing Re/L and h/δ.

Control force values calculated for $h > 1.5\delta$ for the step model of Zukoski[4] and the jet interaction model of Werle et al.[6]

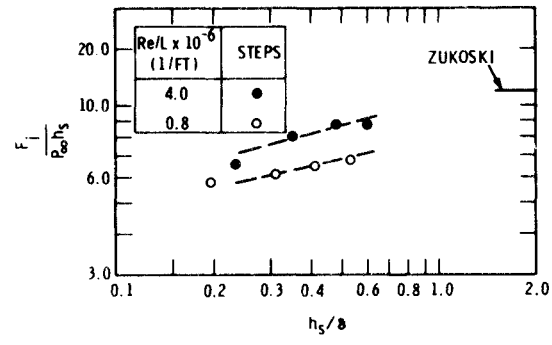

Fig. 4 Dimensionless force, evaluated by integrating the pressure distributions, compared with Zukoski's approximation for $h_s/\delta \geq 1.5$.

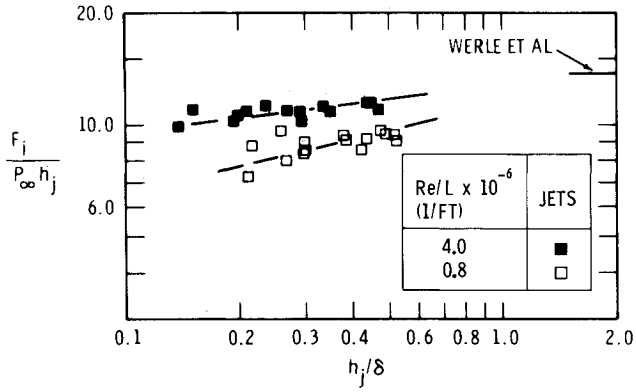

Fig. 5 Dimensionless force, evaluated by integrating the pressure distributions, compared with Werle's approximation for $h_j/\delta \geq 1.5$.

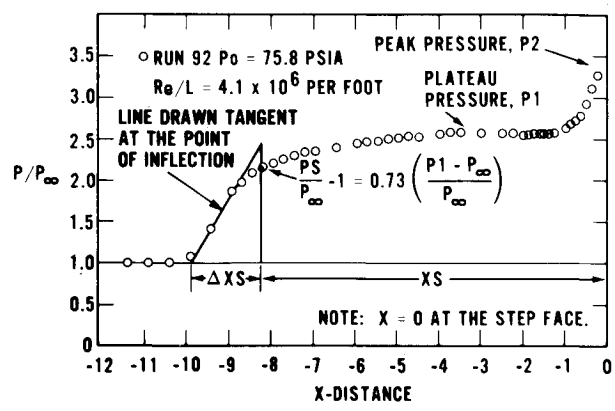

Fig. 7 Typical step pressure distribution.

are also presented, respectively, on Figs. 4 and 5. As mentioned previously in the Introduction, the essential difference between these two force models is the step height to jet height ratio, h_s/h_j. For $h/\delta > 1.5$, Werle[6] found this ratio to be $h_s/h_j = 1.36$. The four curves presented in Fig. 6 represent all of the experimental results listed in Tables 1 and 2. These results indicate that

$$h_s = 1.5h_j \tag{4}$$

is a reasonable approximation which compares favorably with the result of Ref. 6.‡

Discussion of Results

Werle et al.[6] demonstrated that for $h > \delta$ a universal correlation existed for step-induced and jet-induced separation pressure distributions. In their correlation the fraction of plateau pressure rise, $(P-P_\infty)/(Pl-P_\infty)$, was plotted against the fraction of separation distance, X/XS. A similar correlation was sought for the present data. Use of the oil flow separation data did not produce the desired correlation distance. It was found, though, that a (turbulent) separation criterion developed by Zukoski[4] would correlate the present data between $X = 0$ and $X = XS$, the point defined by the criterion. According to this criterion, the separation pressure rise $(PS-P_\infty)$ is 73% of the plateau pressure rise $(Pl-P_\infty)$.§ For values of X greater than XS, the correlation scheme using XS failed to establish the desired universal pressure profile. This failure naturally forces one to consider the problem of finding a second normalizing distance which has significance to the initial steep pressure rise region (the upstream region where dP/dX begins to steepen rapidly with distance and separation physically occurs).

A distance called ΔXS was found which proved to be satisfactory. The graphical definition of ΔXS is presented in Fig. 7. As seen, individual values of ΔXS are taken graphically from each individual pressure distribution curve.

The use of XS and ΔXS as scaling lengths completed the universal pressure distribution with the results shown in Fig. 8. To permit both sets of normalizing distances to vary from 0 to 1.0, the point determined by Zukoski's criterion was established as the point $X = 0$. Figures 8a–8f are the normalized results of Figs. 2 and 3 taken in sequence. The six distributions appear to be of the same parent population and are adequately represented by the single curve of Fig. 8g labeled "universal curve."

As a result of using the graphical definition for ΔXS, the universal curve of Fig. 8g does not pass through a zero point at $X/\Delta XS = 1$. This introduces a very small error into the integrated value for α (defined on Fig. 8g). To remove this small error would require the redefinition of ΔXS, i.e., by redefining the distance ΔXS as starting at a point further upstream where the pressure rise first begins. Experimentally this point is difficult to determine. Knowledge of the location of the precise beginning of the pressure rise is not always known or even available. On the other hand, the gross features of most pressure distribution data would allow one to establish a slope at the point of inflection and hence a value for ΔXS as defined in Fig. 7. This graphical technique was in fact applied to the published data of Bogdonoff.[11] The results are presented in Fig. 8g as the shaded area. The agreement appears reasonable, considering that Bogdonoff's data was taken with steps which extended to the wind-tunnel side walls as opposed to steps with end plates. For these reasons the graphical definition of ΔXS was used.

The existence of a universal pressure profile implies that the

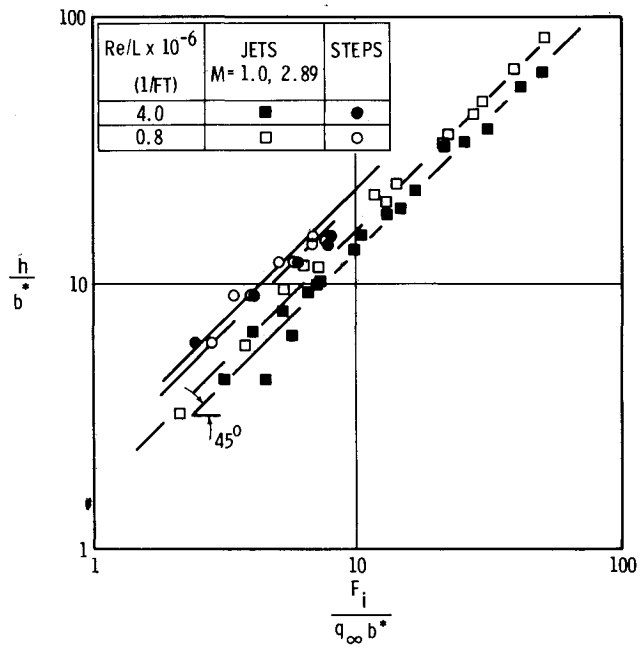

Fig. 6 Equivalent jet heights.

‡ Since the results of Fig. 6 are independent of b^*, the value of $b^* = 0.1$ in. was arbitrarily used by the author to shift the step data to the same logarithmic range with the actual jet data.

§ A word of caution is necessary relative to the interpretation one should apply to the distance, XS. XS as used with the present data should not be considered to be anything other than a definitive "scale change point" for two reasons. First, the "true separation point" was not experimentally measured by any means other than by oil flow. Second, the original basis for the separation criterion of Zukoski rests upon step separation data for which $h > \delta$.

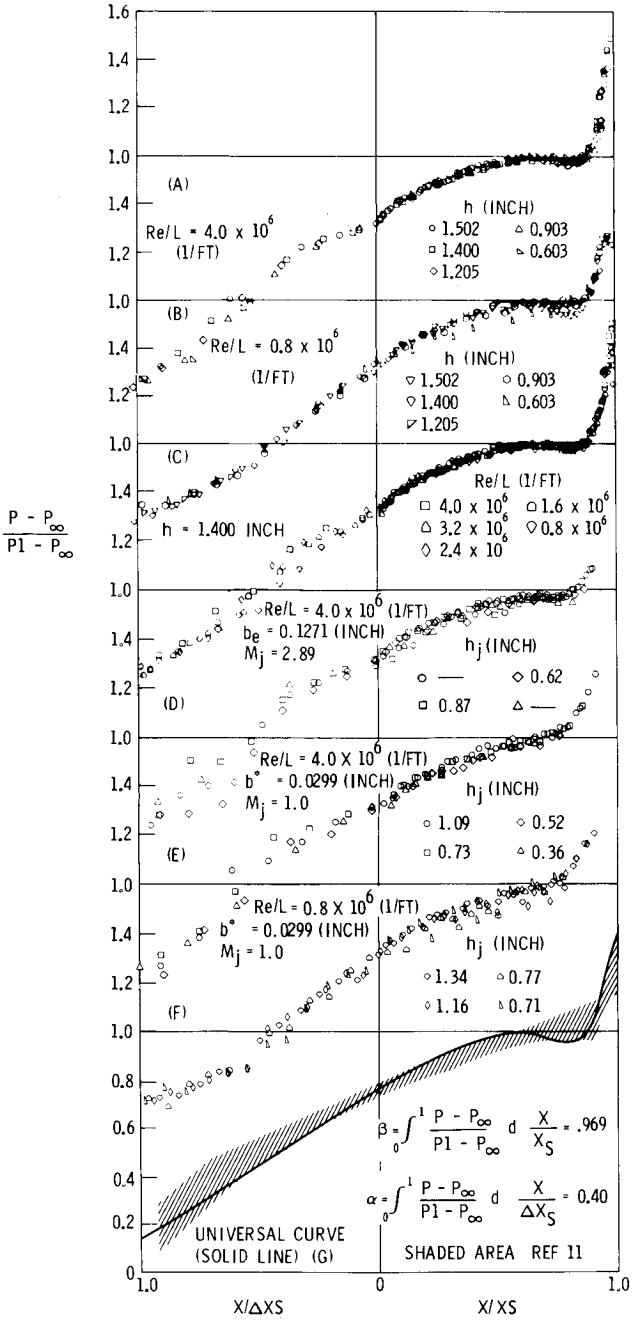

Fig. 8 Universal pressure profiles ahead of forward facing steps and ahead of interacting jets.

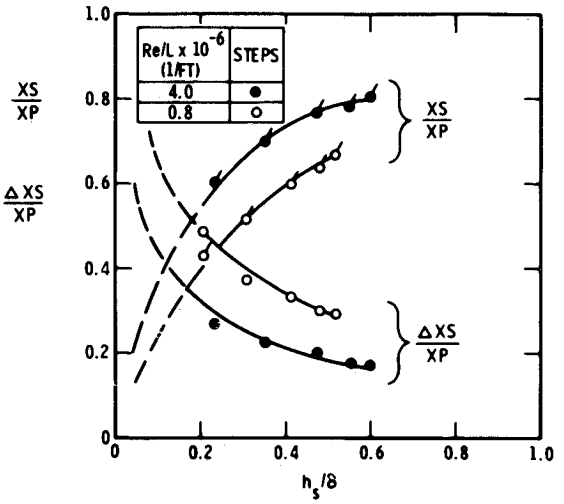

Fig. 9 Functional dependence of the geometric parameters, XS/XP and $\Delta XS/XP$ with h_s/δ and Re/L.

functional dependence of the pressure distributions on Re/L and h/δ (see Figs. 2 and 3) is now incorporated in the scale parameters ΔXS and XS. To investigate this functional dependence, a third distance called the projected shock distance, XP, was defined. As the name implies, the projected shock distance is the distance measured from the step face (or jet slot) to the point on the test plate where the straight-line projection of that part of the separation shock, which is located in the inviscid flowfield, strikes the flat-plate surface. Hence, XP is a distance determined independently of ΔXS and XS. The relationship which exists between these three distances was first determined by investigating the equation

$$D = XP - (\Delta XS + XS) \tag{5}$$

for it was believed that the difference between these quantities would be such that

$$D = D(Re/L, h, \delta, n) \tag{6}$$

where n is the exponent of the turbulent boundary-layer profile. The experimental result of all step data and jet interaction data turned out to be the single straight-line equation.

$$XP = \Delta XS + XS + 1 \text{ (in.)} \tag{7}$$

which implied that this difference, D, is in fact independent of Re/L and h within the range of values covered in this study. Further, since δ experienced only small changes throughout this experimental study and n was nearly constant (see Appendix, Ref. 10), it is logical to assume that

$$D = D(\delta, n) = \text{const} = 1.0 \text{ in.} \tag{8}$$

is a reasonable result.

With XP as a normalizing distance, the ratios $\Delta XS/XP$ and XS/XP may be interpreted as the fraction of the shock projection distance assigned to the initial steep pressure rise process and the fraction of the shock projection distance assigned to the separated region, respectively. For the case of the step, Fig. 9 shows the functional dependence of these fractional distances on h_s/δ for different values of Re/L. Figure 10 shows similar results for the jets. One may reason that as h_s/δ increases without limit, that is, either h_s becomes large or δ becomes small or both, $\Delta XS/XP$ must approach a limit of zero. For the same conditions, XS/XP must approach unity. On the other hand, as h_s/δ decreases, XS/XP must approach zero. An example of this latter case is seen in the pressure distribution of Fig. 2a

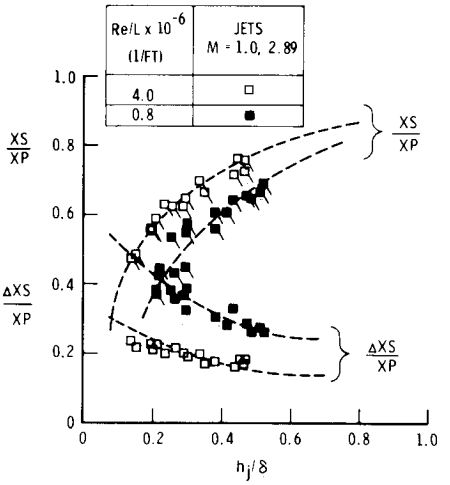

Fig. 10 Functional dependence of the geometric parameters, XS/XP and $\Delta XS/XP$ with h_j/δ and Re/L.

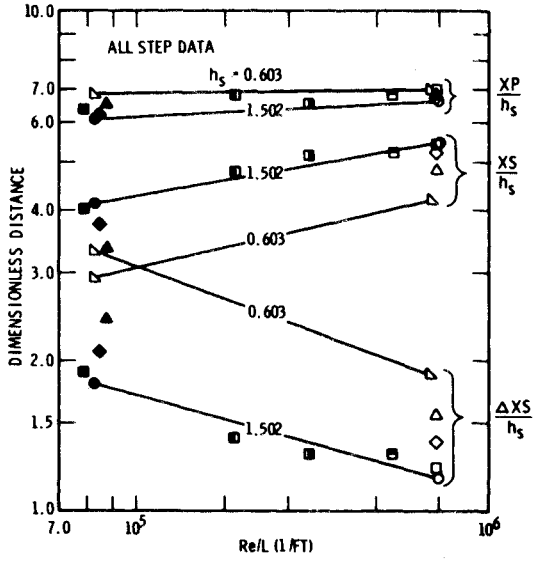

Fig. 11 Dimensionless distances correlated with unit Reynolds number.

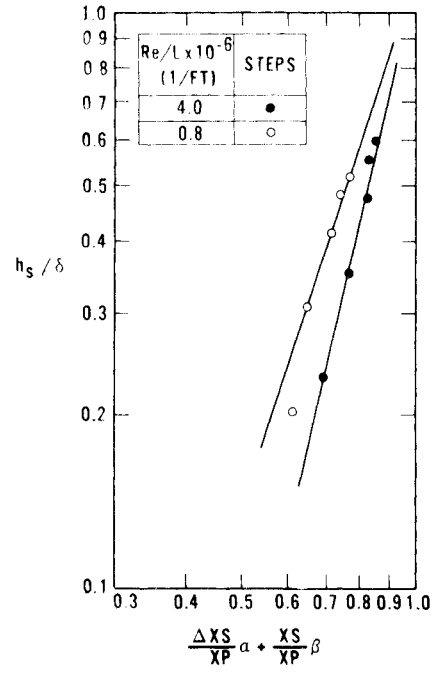

Fig. 13 Variation of the profile coefficient with h_s/δ and Re/L.

for $h_s = 0.247$ in. The limiting behavior of $\Delta XS/XP$ as h_s/δ approaches zero is not known. It is seen experimentally, within the range of experimental data, that $\Delta XS/XP$ increases as h_s/δ decreases.

The variation in the bluntness of the pressure distributions in the initial steep pressure rise region was observed previously in Figs. 2 and 3. Since the magnitude of ΔXS is related to this bluntness (see Fig. 7) by construction and the bluntness appears to vary with Re/L, one would expect that $\Delta XS/XP$ decreases with increasing Re/L (for constant h_s/δ). In the same fashion, XS/XP increases with increasing Re/L (for constant h_s/δ). These two facts are readily verified in Figs. 9 and 10.

Figure 11 presents the geometric parameters $\Delta XS/h_s$, XS/h_s and XP/h_s as functions of Reynolds number per foot. A simple interpretation of the last parameter, XP/h_s, may be made. This parameter establishes the shock standoff distance relative to the step and may be interpreted as the cotangent of the turning angle necessary to produce the oblique shock found in the inviscid flowfield. The proof of this statement is presented in Fig. 12 where a comparison is made between the experimentally measured plateau pressures and those computed using the turning angle consistent with the experimental cotangent, XP/h_s. The data comparison seems to support the interpretation given XP/h_s.

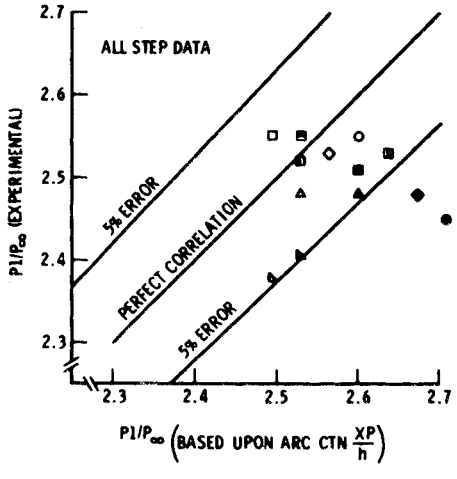

Fig. 12 Experimental plateau pressures compared with calculated values based upon arc ctn (XP/h).

Returning to Fig. 11, the opposite slopes exhibited by $\Delta XS/h_s$ and XS/h_s are such that XP/h_s is observed to be nearly constant for a given value of h_s—a result consistent with Eqs. (5) and (7).

Zukoski[4] reports that the wedge appears to be a reasonable model for the separation region when $h > 1.5\delta$. For this case, the cotangent of the wedge angle is 4.2 (and constant) for fully developed turbulent boundary-layer flow. Note in Fig. 11, XP/h_s is approximately 6.8 for a step of height $h_s = 0.603$ in. ($h_s/\delta \sim 0.2^+$) and 6.3 for a step of height $h_s = 1.502$ in. ($h_s/\delta \sim 0.5^+$). Hence, the experimental trend of XP/h_s tends to agree with Zukoski's prediction as h approaches 1.5δ.

Control Force Considerations

The induced control force due to flow separation may be evaluated as

$$F_i = \int_X (P - P_\infty)\, dX \tag{9}$$

By expanding and normalizing Eq. (9) and introducing the pressure distribution constants, α and β, Eq. (9) can be cast into the following form:

$$\frac{F_i}{P_\infty h_s} = \left(\frac{Pl - P_\infty}{P_\infty}\right)\left(\frac{XP}{h_s}\right)\left(\frac{\Delta XP}{XP}\alpha + \frac{XS}{XP}\beta\right) \tag{10}$$

Note that the first two terms of Eq. (10) are functions of h/δ alone based upon the previously mentioned results of Figs. 2, 3, and 11, while the third term, the pressure profile coefficient, is a function of both Re_δ and h/δ. Experimentally, for $h > \delta$, Eq. (10) must reduce to

$$F_i/P_\infty h_s = [(Pl - P_\infty)/P_\infty]\, XP/h_s \tag{11}$$

as demonstrated by the results of Werle et al.[6] To proceed from Eq. (10) to Eq. (11) requires the pressure profile coefficient to assume the value of 1.0, i.e., become independent of Re_δ and h/δ. Figures 13 and 14 demonstrate this fact adequately for the steps and jets, respectively.

Figure 15 demonstrates the over-all accuracy of these control force calculations. A direct comparison between values determined by integration of the pressure distributions, Figs. 2 and 3, and those calculated using the experimental data and the force model of Eq. (10) is shown for the jet interaction data. This comparison is considered to be satisfactory in view of the fact

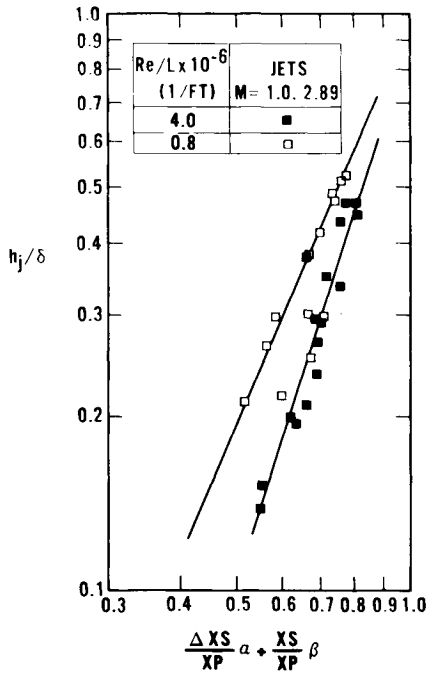

Fig. 14 Variation of the profile coefficient with h_j/δ and Re/L.

that the jet data typically exhibited the greater amount of experimental scatter.

Conclusions

The major result of this two-dimensional flowfield study is the definition of a universal pressure distribution, valid for two-dimensional steps and interacting jets. While this particular study was performed within the dimensionless height range of $0.1 \leqq h/\delta \leqq 0.6$, it was demonstrated that the universal pressure distribution determined in this study includes as a special case the previously reported work of Werle et al.,[6] valid for $h/\delta > 1.5$.

The pressure distributions, (P/P_∞ vs X), measured in the upstream separated region, were found to be functions of both the dimensionless height ratio, h/δ, and the freestream Reynolds number, Re_δ, for the supersonic flow case where $M_\infty = 4.90$.

Three geometric lengths, ΔXS, XS and XP were defined. The ratio, XP/h_s, was interpreted as the cotangent of the wedge angle necessary to produce the plateau pressure, Pl. By definition, XP locates the separation shock in the inviscid flowfield relative to the step face or jet slot. Since the wedge angle is known, the shock angle itself can be computed using the two-dimensional oblique shock relations.

The ratios $\Delta XS/XP$ and XS/XP are indicative of the fractional distances necessary for the occurrence of the initial steep pressure rise and for the extent of the separated region, respectively. This last point should again be qualified though by emphasizing the fact the Zukoski's separation criterion[4] as used for this study locates a point on the pressure signature which must be interpreted as a scale change point, not necessarily a separation point as the title of this criterion would suggest. The separation point per se is not known except by the oil flow.

The difference between XP and the sum $(\Delta XS + XS)$, while a constant for this study, is believed to be functionally dependent upon the actual boundary-layer thickness, δ, and the turbulent boundary-layer profile exponent, n.

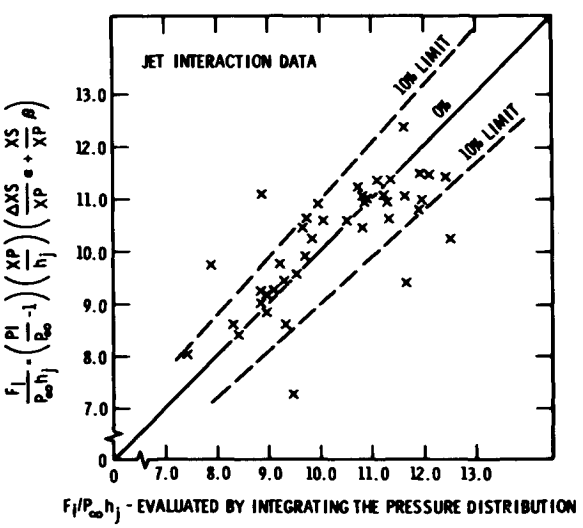

Fig. 15 Comparison of dimensionless force data.

References

[1] Reda, D. C. and Murphy, J. D., "Shock Wave/Turbulent Boundary-Layer Interactions in Rectangular Channels," *AIAA Journal*, Vol. 11, No. 2, Feb. 1973, pp. 139–140.

[2] Reda, C. C. and Murphy, J. D., "Shock Wave/Turbulent Boundary-Layer Interactions in Rectangular Channels, Part II: The Influence of Sidewall Boundary Layers on Incipient Separation and Scale of the Interaction," *AIAA Journal*, Vol. 11, No. 10, Oct. 1973, pp. 1367–1368.

[3] Ryan, B. M., "Summary of Aerothermodynamic Interference Literature," TN 4061-160, April 1969, Naval Weapons Center, China Lake, Calif.

[4] Zukoski, E. E., "Turbulent Boundary-Layer Separation in Front of a Forward-Facing Step," *AIAA Journal*, Vol. 5, No. 10, Oct. 1967, pp. 1746–1753.

[5] Werle, M. J., "A Critical Review of Analytical Methods for Estimating Control Forces Produced by Secondary Injection—The Two-Dimensional Problem," NOLTR 68-5, Jan. 4, 1968, Naval Ordnance Lab., White Oak, Md.

[6] Werle, M. J., Driftmyer, R. T., and Shaffer, D. G., "Two-Dimensional Jet Interaction with a Mach 4 Mainstream," NOLTR 70-50, May 1, 1970, Naval Ordnance Lab., White Oak, Md.

[7] Werle, M. J., Driftmyer, R. T., and Shaffer, D. G., "Jet Interaction Induced Separation: The Two-Dimensional Problem," *AIAA Journal*, Vol. 10, No. 2, Feb. 1972, pp. 188–193.

[8] Hahn, J. S., "Experimental Investigation of Turbulent Step-Induced Boundary-Layer Separation at Mach Numbers 2.5, 3, and 4," AEDC-TR-69-1, March 1969, Arnold Engineering Development Center, Tullahoma, Tenn.

[9] Lee, R. E., Yanta, W. J., Leonas, A. C., and Carner, J. W., "The NOL Boundary Layer Channel," NOLTR 66-185, Nov. 7, 1966, Naval Ordnance Lab., White Oak, Md.

[10] Driftmyer, R. T., "A Forward-Facing Step Study: The Step Height Less than the Boundary-Layer Thickness," NOLTR 73-98, May 1973, Naval Ordnance Lab., White Oak, Md.

[11] Bogdonoff, S. M., "Some Experimental Studies of the Separation of Supersonic Turbulent Boundary Layers," Rept. 336, June 1955, Princeton Univ., Princeton, N.J.